Experimental Study on Propagation Mode of Cylindrical Rotating Detonation Engine with Liquid Ethanol – Liquid Nitrous Oxide

Tomoki Sato[1)], Kazuki Ishihara[1)], Kotaro Nakata[1)], Tomoaki Kimura[1)], Yusei Kikuchi[1)], Kosuke Nakajima[1)], Satoru Sawada[1)], Masahiro Inada[1)], Rinpei Sakata[1)], Yamato Suzuki[1)], Yusuke Oda[1)], Noboru Itouyama[2)], Ken Matsuoka[1)], Jiro Kasahara[2)], Akira Kawasaki[3)], Hiroaki Watanabe[4)], Hiro Okano[5)], Takuya Tada[5)], Akitomo Fujiura[5)], Mio Namera[5)], Ryu Nakazawa[5)], Hikaru Eguchi[5)], Daisuke Nakata[5)], Masaharu Uchiumi[5)], Akiko Matsuo[6)], Ikkoh Funaki[7)]

[1)]Department of Aerospace Engineering, Nagoya University, Nagoya, Japan
[2)]Institute of Materials and Systems for Sustainability, Nagoya University, Nagoya, Japan
[3)]Department of Mechanical Engineering, Shizuoka University, Hamamatsu, Japan
[4)]Department Fluides, Thermique et Combustion, ENSMA, Chasseneuil du Poitou, France
[5)]Aerospace Plane Research Center, Muroran Institute of Technology, Muroran, Japan
[6)]Department of Mechanical Engineering, Keio University, Yokohama, Japan
[7)]JAXA Institute of Space and Astronautical Science, Sagamihara, Japan

1 Introduction

Detonation wave is a supersonic combustion wave propagating in combustible mixtures (Mach number about 4 to 7) accompanied by shock waves [1]. Detonation waves can complete combustion in an extremely short period of time due to fluid compression to high temperatures and pressures by the shock wave. Therefore, a combustor using detonation waves has many advantages that is very short combustor and higher theoretical thermal efficiency than conventional combustors. One of the combustors using detonation wave is a rotating detonation engine (RDE), in which detonation waves are propagated circumferentially inside the combustor to produce work in the axial direction [2].

In recent studies toward practical use of aerospace propulsion, RDE using gaseous methane and gaseous oxygen as propellants developed by our research group was successfully demonstrated in space at an altitude of over 150 km using sounding rocket S-520-31 on July 27 in 2021 [3]. Moreover, M. Kawalec et al. demonstrated RDE flight test using liquid propane and liquid nitrous oxide with regenerative cooling. This is first RDE flight powered by liquid propellant [4].

Our research group studies on a bipropellant cylindrical RDE with liquid ethanol and liquid nitrous oxide as propellants further practical space application of RDEs. In this paper, the operating condition and effect of propellant temperature are reported.

Correspondence to: sato.tomoki.s7@s.mail.nagoya-u.ac.jp

2 Experimental setup

Figure 1(a) shows a schematic view of an experimental setup in this study. The combustor length L_c was 130 mm, and the inside diameter was φ40.0 mm. The nozzle throat diameter was φ30.5 mm and the nozzle exit diameter was φ61.0 mm or φ92.0 mm. The propellants were liquid ethanol and liquid nitrous oxide. Both were supplied by nitrogen pressurization. For thermal protection by longer combustion, carbon fiber reinforced carbon(C/C) was used. The injectors are remade for longer combustion although each geometry is the same. In this study, pressure, temperature, and thrust were measured. Pressure sensors (Keller, PA-23) were installed at the bottom of the combustor (injector surface) and on the combustor wall. Temperatures were installed in the liquid fuel and oxidizer manifold. A high-speed camera was used to visualize the inside of the combustor. The high-speed camera was used at a frame rate of 400,000 fps and 0.4 µs exposure. Gun-powders were used for ignition near the combustor bottom. Experiments were conducted under atmospheric pressure.

Figure 1(b) shows an overview near the injector. The injector is an unlike impinging type for vaporization of nitrous oxide near the injector. The liquid oxidizer and liquid fuel injectors were spaced at φ21 mm and φ27 mm from the combustor center, respectively, and collided at 1.5 mm from the bottom. The liquid fuel injector has a straight hole type of 48×φ0.25 mm, and each liquid oxidizer injector has the same type of 48×φ0.35 mm.

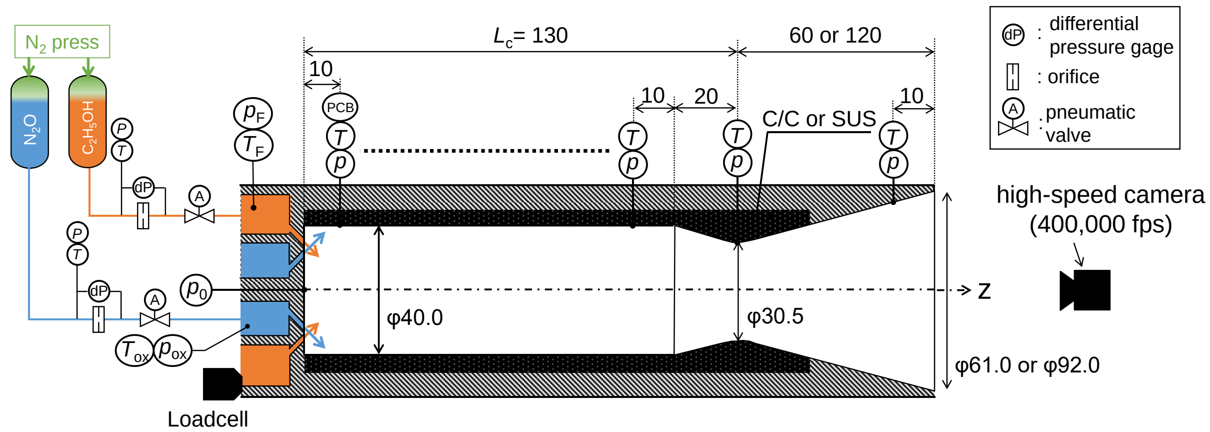

(a) The schematic view of an experimental setup

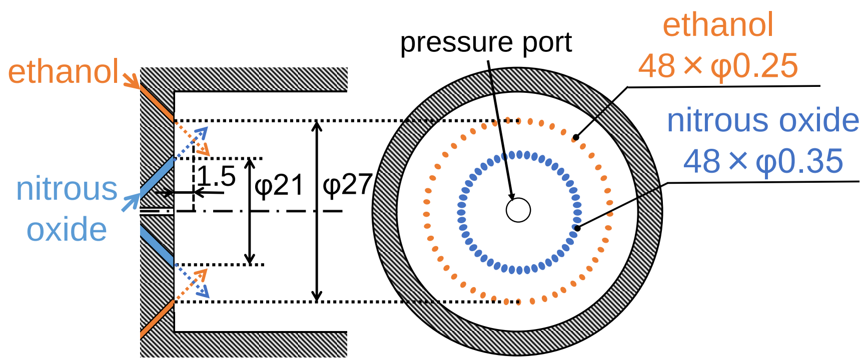

(b) The overview of injectors

Figure 1 The schematic view of an experimental setup;
(a) schematic view of RDE, (b) the overview of injectors

Table 1 Experimental conditions and summary of results

shot num.	combustion mode	wall	operation time t_{ope} [s]	nitrous oxide manifold temperature $T_{N2O,mani}$ [°C]	ethanol manifold temperature $T_{EA,mani}$ [°C]	total mass flow rate $\dot{m}_{tot}$ [g/s]	mixture ratio O/F [-]	Thrust F_{exp} [N]	specific impulse $I_{sp,exp}$ [s]
#01	detonation	SUS	1.14	28.0 ± 1.2	29.4 ± 0.2	185.3 ± 2.1	5.08 ± 0.10	233 ± 13	128 ± 8
#02	detonation	SUS	1.13	23.8 ± 1.1	24.5 ± 0.1	198.4 ± 2.1	4.53 ± 0.09	290 ± 15	149 ± 8
#03	detonation	SUS	1.13	27.2 ± 1.6	26.6 ± 0.1	193.3 ± 2.5	4.26 ± 0.10	273 ± 15	144 ± 8
#04	detonation	SUS	1.13	27.0 ± 1.1	28.0 ± 0.1	197.7 ± 2.6	4.09 ± 0.09	280 ± 14	144 ± 8
#05	deflagration	SUS	1.13	27.4 ± 1.3	28.6 ± 0.1	202.9 ± 3.3	3.70 ± 0.10	287 ± 15	144 ± 8
#06	deflagration	SUS	1.01	-4.00 ± 0.28	-1.98 ± 0.10	207 ± 18	5.53 ± 0.75	284 ± 18	140 ± 15
#07	deflagration	SUS	5.03	-0.94 ± 0.06	1.30 ± 0.01	196.1 ± 8.8	4.74 ± 0.38	271 ± 10	141 ± 7
#08	deflagration	C/C	15.1	6.77 ± 0.46	0.87 ± 0.05	190.7 ± 6.6	4.35 ± 0.20	259 ± 7	139 ± 6
#09	deflagration	C/C	15.1	16.8 ± 1.2	0.40 ± 0.02	176 ± 12	3.32 ± 0.37	173 ± 9	100 ± 8

3 Results and Discussions

A summary of the experimental conditions and a summary of the experimental results are shown in Table 1. Throughout the experiment, the total mass flow rate $\dot{m}_{tot}$ was 176~203 g/s, mixture ratio O/F was 3.32~5.53. From the propellant temperature as shown in Table 1, combustion tests were conducted in different seasons (#01~#05 were tested in summer and #06~#09 were tested in winter). Since the total mass flow rate and mixture ratio were the same value, the pressure of each tank is different between #01~#05 and #06~#09 because of different vapor pressure.

Figure 2 shows typical thrust, mass flow rate, mixture ratio, pressure, and temperature history. As shown in Figure 2, thrust and pressure are almost constant during combustion test in shot #1, but thrust decreases in shot #9. This is thought to be because the liquid temperature of nitrous oxide rises and easily evaporates near the injector, thus decreasing the total flow rate. The following typical values are the values averaged near the end of the combustion test as shown by the yellow region in Figure 2.

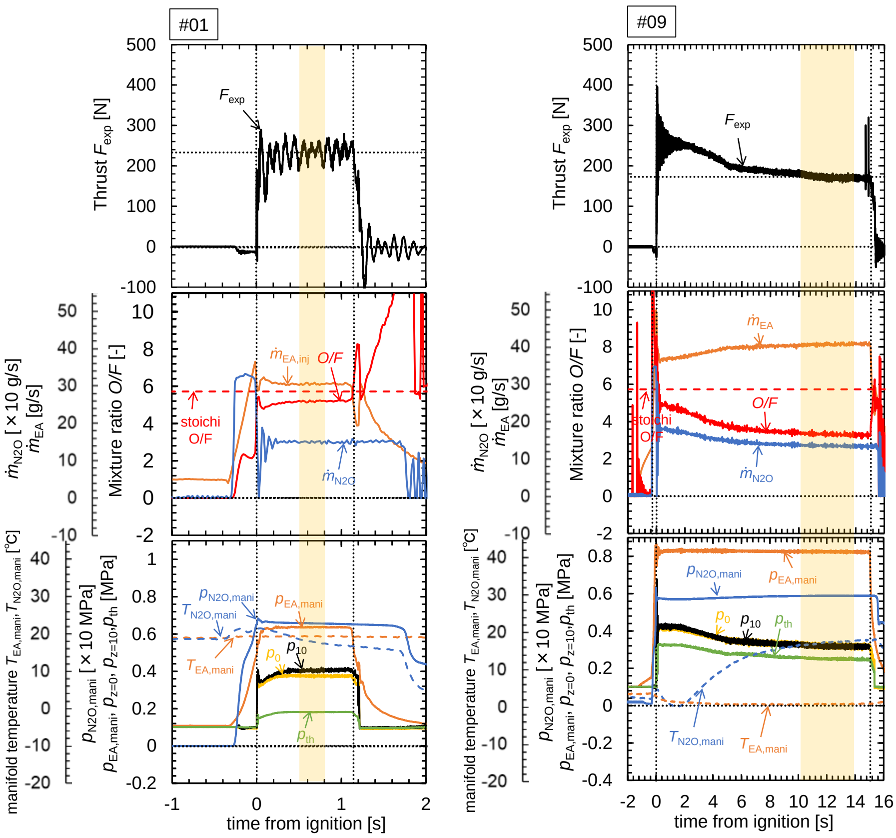

Figure 2 **Typical thrust, mass flow rate, mixture ratio, pressure, and temperature history.**

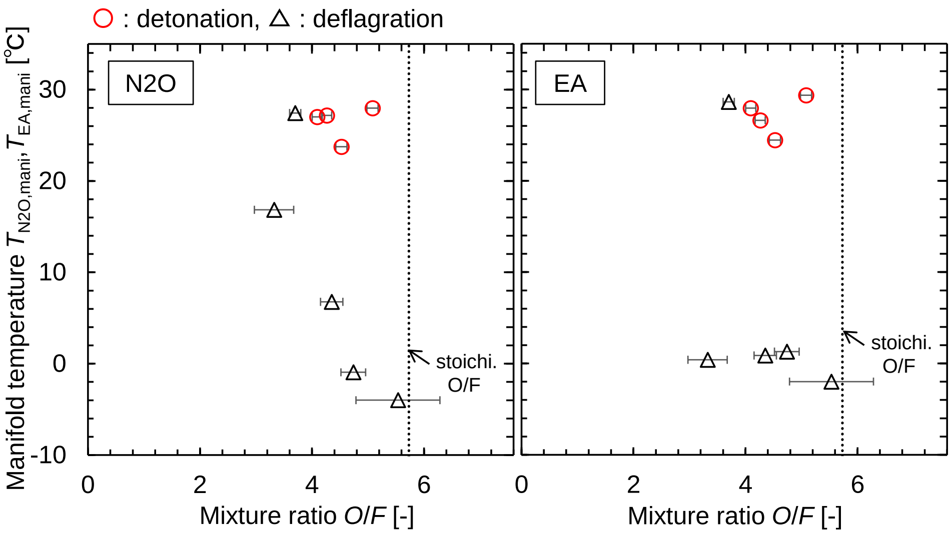

Figure 3 **The effect of manifold temperature and mixture ratio on propagation mode.**

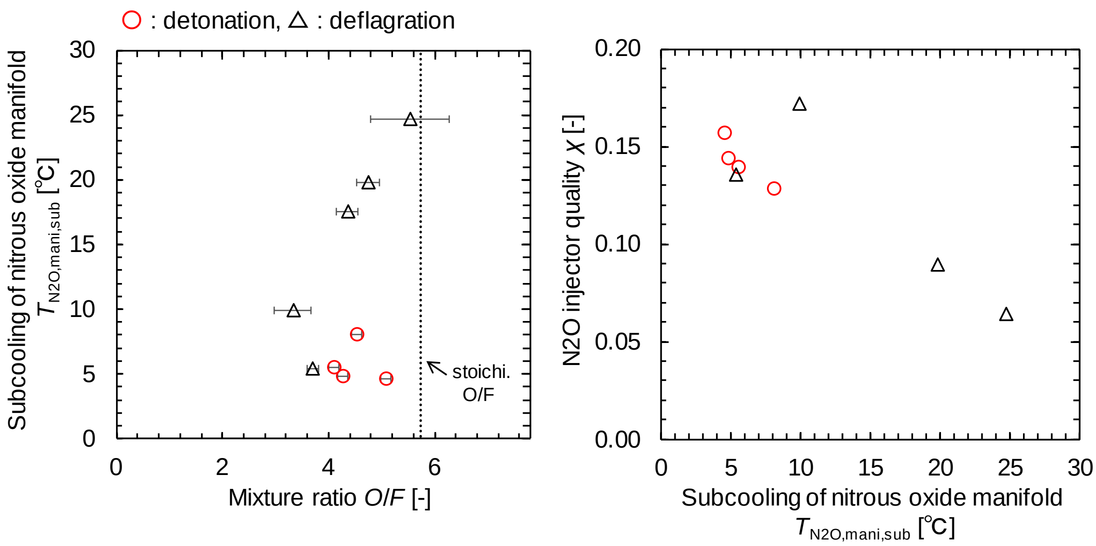

Figure 4 **The effect of subcooling degree and injector quality on propagation mode.**

Figure 3 shows the effect of manifold temperature and mixture ratio on propagation mode. As shown in Figure 3, detonation did not occurred without a limited range of mixture ratio. Moreover, the manifold temperature of each propellant has an effect on the propagation mode. It is thought that the lower liquid temperature makes it more difficult to evaporate and thus difficult to transition to detonation.

Figure 4 shows the effect of subcooling degree and a quality of N_2O injector on propagation mode. Introduce a void function α, which represents the ratio of a injected area of gas to a injector cross-sectional area (Eq.(1)). Moreover Eq.(2) shows a injector quality, which represents a ratio of a gaseous mass flow rate to a total mass flow rate of N_2O injector.

$$\alpha = \frac{A_{\mathrm{g,inj}}}{A_{\mathrm{inj}}} \tag{1}$$

$$\chi = \frac{\dot{m}_{\mathrm{g,inj}}}{\dot{m}_{\mathrm{tot}}} \tag{2}$$

Eq.(3) shows a mass flow rate when total mass flow rate is supplied as a liquid form, and Eq.(4) shows a mass flow rate when total mass flow rate is supplied as a gaseous form.

$$\dot{m}_{\mathrm{L,inj,all}} = C_{\mathrm{d,O,inj}} \cdot N_{\mathrm{O,inj}} \frac{d_{\mathrm{O,inj}}^2}{4} \pi \cdot \sqrt{2 \cdot \rho_{\mathrm{O,mani}} \cdot (p_{\mathrm{O,mani}} - p_0)} \tag{3}$$

$$\dot{m}_{\mathrm{g,inj,all}} = C_{\mathrm{d,O,inj}} \frac{p_{\mathrm{O,mani}} \cdot N_{\mathrm{O,inj}} \frac{d_{\mathrm{O,inj}}^2}{4} \pi}{\sqrt{R_{\mathrm{O,mani}} T_{\mathrm{O,mani}}}} \sqrt{\gamma_{\mathrm{O,mani}} \left(\frac{2}{\gamma_{\mathrm{O,mani}} + 1} \right)^{\frac{\gamma_{\mathrm{O,mani}}+1}{\gamma_{\mathrm{O,mani}}-1}}} \tag{4}$$

In this case, the actual mass flow rate $\dot{m}$ is the sum of the liquid mass flow rate $\dot{m}_{\mathrm{L,inj}}$ and the gaseous mass flow rate $\dot{m}_{\mathrm{g,inj}}$, which is expressed in Equation (5).

$$\begin{aligned} \dot{m}_{\mathrm{ori}} = \dot{m}_{\mathrm{L,inj}} + \dot{m}_{\mathrm{g,inj}} &= C_{\mathrm{d,O,inj}} \rho_{\mathrm{L,inj}} u A_{\mathrm{L,inj}} + C_{\mathrm{d,O,inj}} \rho_{\mathrm{g,inj}} u A_{\mathrm{g,inj}} \\ &= (1-\alpha) C_{\mathrm{d,O,inj}} \rho_{\mathrm{L,inj}} u A_{\mathrm{inj}} + \alpha C_{\mathrm{d,O,inj}} \rho_{\mathrm{g,inj}} u A_{\mathrm{inj}} \\ &= (1-\alpha) \dot{m}_{\mathrm{L,inj,all}} + \alpha \dot{m}_{\mathrm{g,inj,all}} \end{aligned} \tag{5}$$

Therefore, since α can be obtained from Eq.(5), χ can be also calculated from Eq.(6).

$$\chi = \frac{\dot{m}_{\mathrm{g,inj}}}{\dot{m}_{\mathrm{ori}}} = \frac{\alpha \dot{m}_{\mathrm{g,inj,all}}}{\dot{m}_{\mathrm{ori}}} \tag{6}$$

As shown in Figure 4, when the subcooling degree of N_2O injector increases, the injector quality decreases. One of the reasons why detonation did not occur is considered that the percentage of vaporized propellant was small. Therefore, there is the effect of the of temperature each propellant and the quality of N_2O injector on propagation mode.

Figure 5 shows experimental specific exhaust velocity c* and comparison of theoretical value. Experimental c* is calculated by Eq.(7), and the theoretical c* is calculated by Eq.(8).

$$c_{\mathrm{exp}}^* = \frac{p_{\mathrm{z,max}} A_{\mathrm{t}}}{\dot{m}_{\mathrm{tot}}} \tag{7}$$

$$c_{\mathrm{th}}^* = \frac{\sqrt{\gamma_{\mathrm{c}} R_{\mathrm{c}} T_{\mathrm{CJ}}}}{\gamma_{\mathrm{c}} \sqrt{\left(\frac{2}{\gamma_{\mathrm{c}} + 1} \right)^{\frac{\gamma_{\mathrm{c}}+1}{\gamma_{\mathrm{c}}-1}}}} \tag{8}$$

As shown in Figure 5, the combustion efficiency was almost the same for detonation and deflagration. However, in the test that the mixture ratio is much lower than the stoichiometric value(shot #9), the combustion efficiency is low. From Figure 2, change in the manifold temperature of liquid nitrous oxide and mixture ratio during the combustion test may be related to this low combustion efficiency.

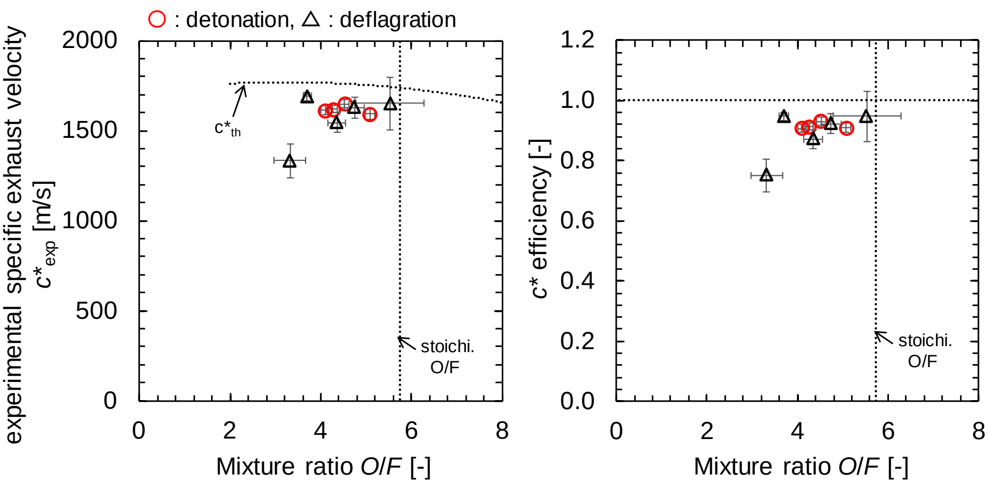

Figure 5 **Experimental c* and comparison of theoretical value.**

4 Conclusions

In this study, a cylindrical rotating detonation combustor was used with liquid ethanol as fuel and liquid nitrous oxide as oxidizer when the total mass flow rate $\dot{m}_{tot}$ was 176~203 g/s, mixture ratio *O/F* was 3.32~5.53 under atmospheric pressure. The following conclusions were obtained.

Detonation was not observed when the temperature of liquid propellant is low. It is thought that the lower liquid temperature makes it more difficult to evaporate and thus difficult to transition to detonation. Moreover, when the subcooling degree of N_2O injector increased, the injector quality decreased. It is considered that detonation was difficult to occur because the percentage of vaporized propellant was small. Therefore, there is the effect of each propellant temperature and the quality of N_2O injector on propagation mode.

In combustion performance, the combustion efficiency was almost the same for detonation and deflagration. However, change in the manifold temperature of liquid nitrous oxide during the combustion test may be related to this low combustion efficiency.

Acknowledgments

This study was financially supported by JSPS KAKENHI Grants No. JP19H05464; and by the Institute of Space and Astronautical Science of the Japan Aerospace Exploration Agency.

This experiment is carried out at the Aerospace Plane Research Center in Shiraoi. The authors are also deeply grateful to all the faculty members and students who have supported this study, including the Muroran Institute of Technology and Nagoya University.

References

[1] John H.S. Lee, "The detonation phenomenon," Cambridge University Press, 2008.

[2] B. A. Rankin, T. A. Kaemming, S. W. Theuerkauf, and F. R. Schauer, "Overview of Performance, Application, and Analysis of Rotating Detonation Engine Technology," J. Propul. Power, Vol. 33, No. 1, 2017.

[3] Goto, K., Matsuoka, K., Matsuyama, K., Kawasaki, A., Watanabe, H., Itouyama, N., Ishihara, K., Buyakofu, V., Noda, T., Kasahara, J., Matsuo, A., Funaki, I., Nakata, D., Uchiumi, M., Habu, H., Takeuchi, S., Arakawa, S., Masuda, J., Maehara, K., Nakao, T., and Yamada, K.: Space Flight Demonstration of Rotating Detonation Engine Using Sounding Rocket S-520-31, Journal of Spacecraft and Rockets, 60(1), 2023, 273-285.

[4] Kawalec, M., Perkowski, W., Łukasik, B., Bilar, A., and Wolański, P., "Applications of the continuously rotating detonation to combustion engines at the Łukasiewicz-Institute of Aviation. Combustion Engines," 61, 2022.